U. S. GEOLOGICAL SURVEY.

REPORTS - OPEN FILE SERIES, no. 1046, 1968.

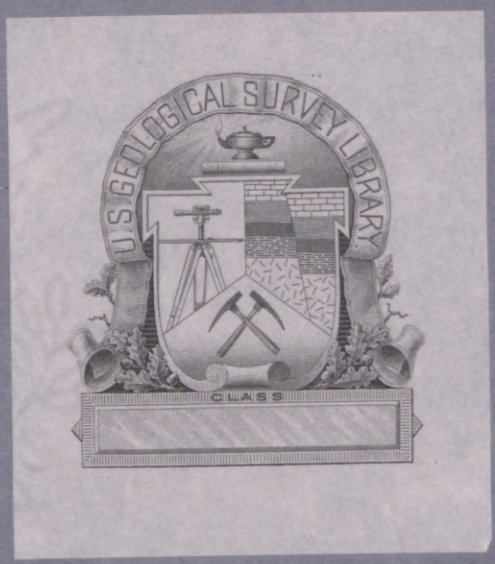
U.S. GEOLOGICAL SURVEY LIBRARY
CLASS

UNITED STATES DEPARTMENT OF THE INTERIOR
GEOLOGICAL SURVEY

APPLICATION OF DISLOCATION THEORY TO ANALYSIS OF VERTICAL DISPLACEMENTS AT THE GROUND SURFACE CAUSED BY THE DURYEA EVENT

by

G. E. Brethauer

Open-file Report
1968

UNITED STATES
DEPARTMENT OF THE INTERIOR
GEOLOGICAL SURVEY

APPLICATION OF DISLOCATION THEORY TO ANALYSIS OF VERTICAL DISPLACEMENTS AT THE GROUND SURFACE CAUSED BY THE DURYEA EVENT

by

G. E. Brethauer

Abstract

Dislocation theory is used in an analysis that explains measured vertical displacements across a fault near the Duryea underground nuclear explosion. The difference between the measured vertical displacement and the theoretically predicted vertical displacement caused by cavity formation is termed the residual vertical displacement. The residual vertical displacement is, therefore, assumed to be the result of faulting triggered by the explosion. The final fault model required by dislocation theory to predict the displacement due to faulting has the following dimensions:

1. Depth to bottom of fault plane: 1,800 feet
2. Depth to top of fault plane: 0 feet
3. Strike length of fault plane: 2,400 feet
4. Dislocation on west side of fault F-1: -1.85 feet
5. Dislocation on east side of fault F-1: -0.14 foot

Introduction

The Duryea explosion, in U20a, was at a depth of 1,795 feet in a rhyolite flow in Pahute Mesa, Nevada Test Site. The areal geology and the geologic effects of the explosion have been described in previous reports by Byers and Cummings (1967) and Ekren (1966), and they have been studied by W. L. Emerick, K. A. Sargent, R. H. Morris, P. J. Barosh, F. A. McKeown, and D. L. Hoover (written communs., 1963, 1965, 1966). The lithology of the U20a emplacement hole was studied by D. L. Hoover, J. W. Hasler, R. P. Snyder, and E. F. Monk (written communs., 1964), and it was summarized by P. P. Orkild (written commun., 1966).

As part of the study of the geologic effects of the Duryea event a second-order level-line survey of 13 stations was made by Holmes & Narver, Inc. at the request of the U.S. Geological Survey. The raw data from this survey were reported by P. J. Barosh, F. A. McKeown, and D. L. Hoover (written commun., 1966). These survey data, as well as much other survey data obtained for other events, may be used to calculate the fault movements that are caused by underground nuclear explosions.

Dislocation theory can be used to calculate the displacements around a fault by using knowledge of the following fault parameters: DLIT, the depth below the surface to the top of the fault plane; DBIG, the depth below the surface to the bottom of the fault plane; 2L, the length of the fault plane; and W, the relative dislocation on the surface at the midpoint of the length of the fault plane. Figure 1 is a diagram of a fault model with these parameters except for W; the fault plane is vertical. The midpoint of the fault plane on the surface will be the origin of a rectangular Cartesian coordinate system used in a mathematical fault model describing the direction and amount of displacement produced by assumed amounts of dislocation at the fault. DBIG, DLIT, and coordinates of surface points in the field around the fault have dimensions in terms of L, the half-length of the fault. The displacements at points on the surface around the fault are given as a fraction of twice the dislocation, W, on one side of the fault plane.

The faults in the vicinity of the Duryea event and the locations of the level-line stations are shown in figure 2. The raw displacement data are shown in figure 3. These vertical displacements could have been caused by the formation of an explosion-cavity, cavity collapse, or movement along a nearby fault.

The operation of one or more of these mechanisms must be assumed in order to explain the displacements.

Upward displacement can be attributed to cavity formation and/or faulting. Downward displacement can be attributed to cavity collapse and/or faulting.

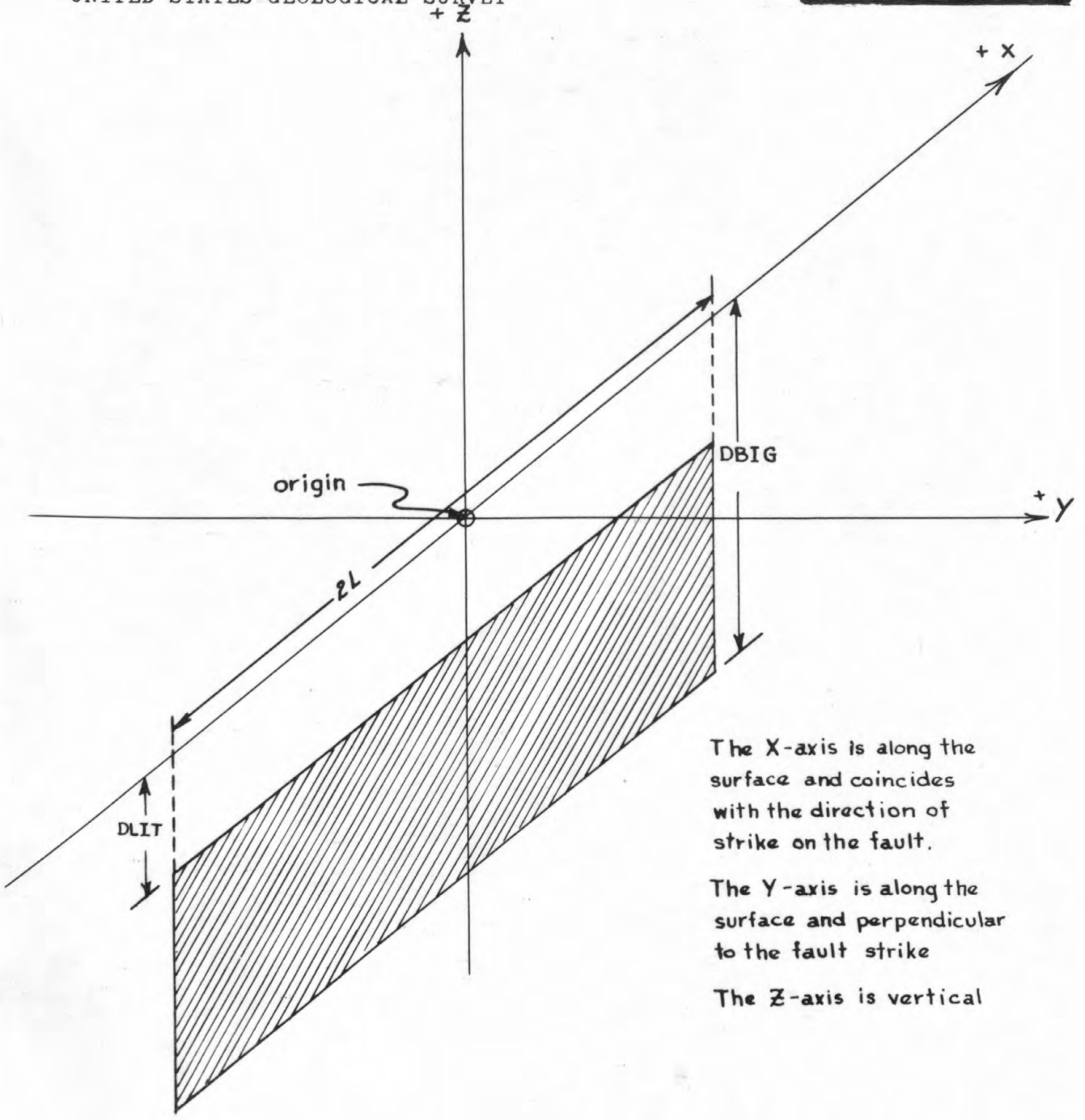

Figure 1.--Schematic diagram of fault model used in dislocation theory with labeled dimensions

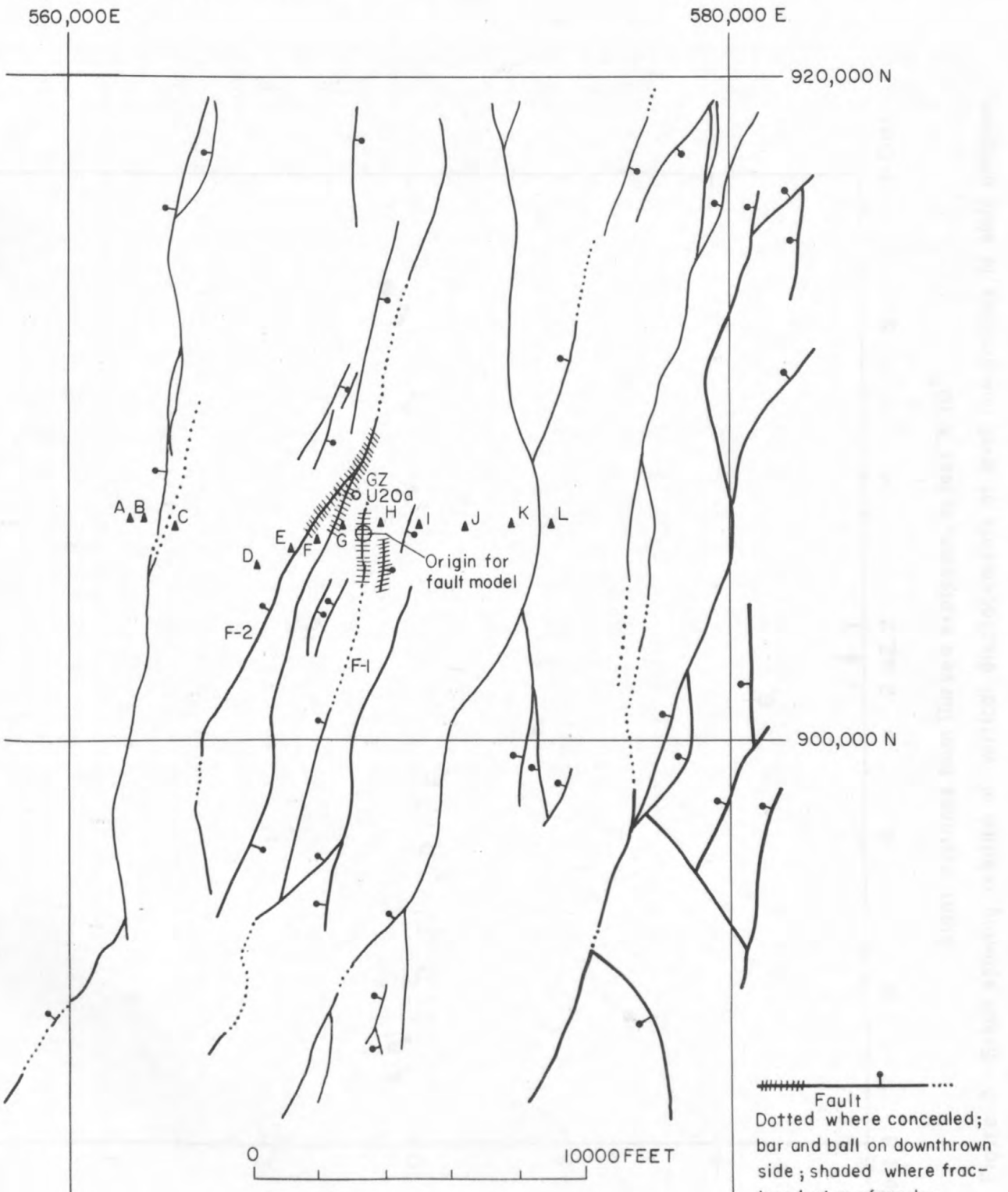

Figure 2.–Map showing faults in vicinity of U20a ground zero (GZ), fracturing along faults, and level-line stations (labeled A through L)

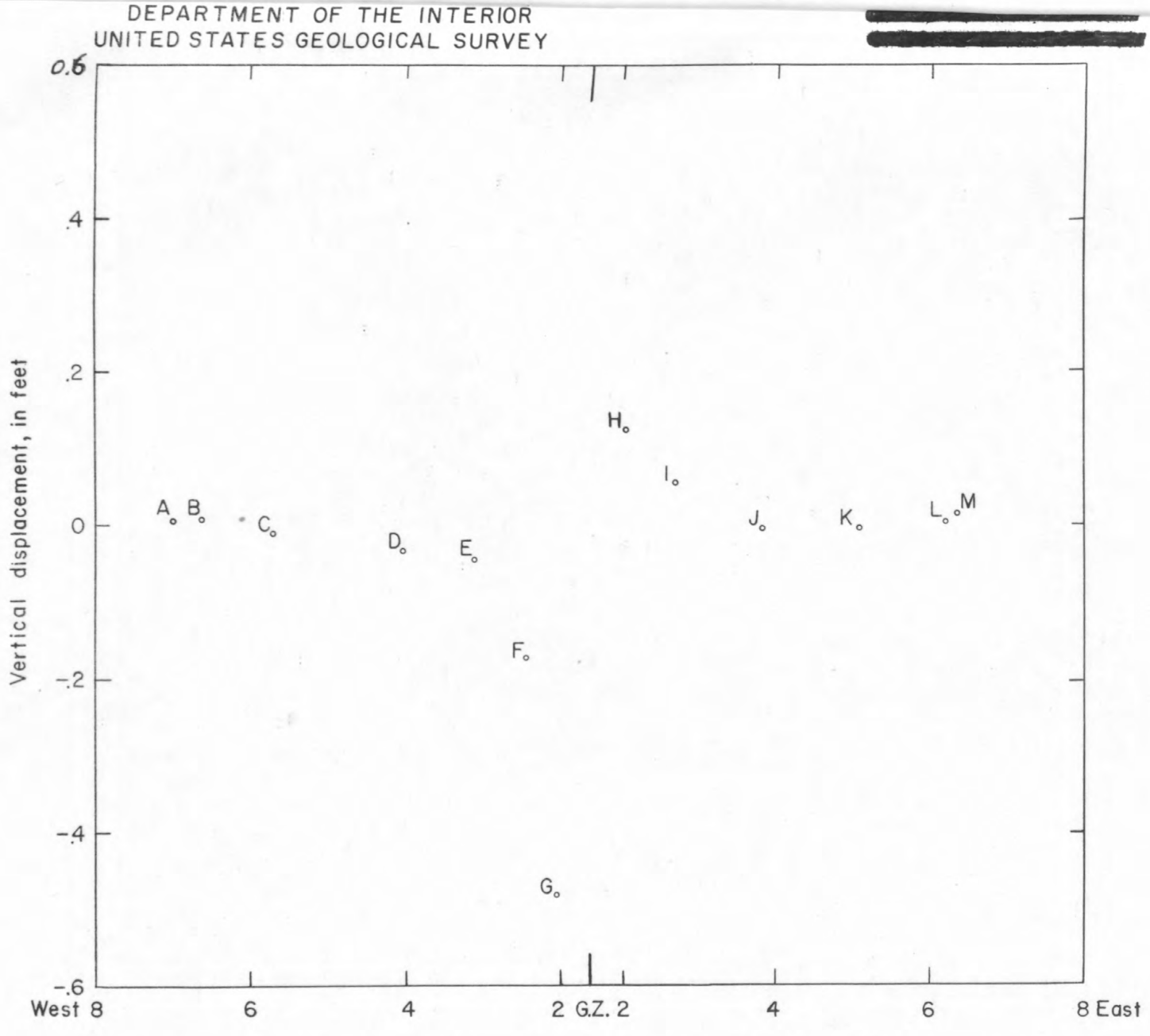

Figure 3. -Graph showing relation of vertical displacements at level line stations to slant distance from Duryea explosion

Downward displacement at the stations, resulting from cavity collapse, can be shown to be analytically unimportant by the following logic: If cavity collapse caused downward displacement near ground zero, the displacement at station H also should be downward as the displacement is at station G (fig. 3). If it is assumed that the intervening fault F-1 (fig. 2), between GZ and station H caused termination of the displacement resulting from cavity collapse, then it is reasonable to assume that displacements at stations F, E, D, and C could not be due to cavity collapse because of the intervening faults, F-2 and its branches, that lie between GZ and these stations. Thus faulting must be used to explain the downward displacement at stations F, E, D, and C. Because no sink formed, cavity collapse fails to explain the displacements at all stations, and the mechanism of cavity collapse would appear to have small effect on displacement at the stations.

In this analysis surface vertical displacements are calculated assuming that measured displacements at the stations were caused by a combination of two mechanisms: cavity formation and faulting. Surface radial displacements due to cavity formation are calculated using an equation describing volume relations between spheres whose centers are at the explosion point.

$$\frac{4\pi}{3}\left(R_f(\theta)\right)^3 = \frac{4\pi}{3}\left(R_p(\theta)\right)^3 - \frac{4\pi}{3}\left(R_i(\theta)\right)^3 \qquad (1)$$

where

θ = angle between any ray, from the explosion point to any given position, and the horizontal

$R_f(\theta)$ = final cavity radius at the angle θ

$R_p(\theta)$ = radius at an angle θ to any point p after the explosion

$R_i(\theta)$ = radius at an angle θ to any point i before the explosion

If $R_p(\theta)$ and $R_i(\theta)$ are assumed to terminate at the surface at angle θ after and before the explosion, respectively, then $(R_p(\theta) - R_i(\theta))$, is termed ΔR, and the vertical surface displacement calculated using equation (1) will be

$$\Delta V = \Delta R \sin\theta = \frac{\left[R_f(\theta)\right]^3}{3\left[R_i(\theta)\right]^2} \sin\theta \qquad \text{for } (R_i(\theta) > 3\,R_f(\theta)) \qquad (2)$$

ΔV = vertical displacement due to cavity formation θ on the surface at a position determined by the intersection of a ray emanating from the explosion center at angle θ and the surface.

If cavities produced by explosions are spherical, $R_f(\theta)$ will be the same for all θ. It is probable that the cavities produced by explosions are not spherical, but ellipsoidal. Cavity radii at different angles from the horizontal would have different lengths. A method of calculating the radius of the ellipsoidal cavity at any angle θ has been described (Brethauer, 1968). Only the final equation for the case where the cavity is confined to one layer of material is given here.

$$R_f(\theta) = R_f(\phi)\left[\frac{1}{1 - \dfrac{\rho_{(m)}\, R_f(\phi)\sin\theta}{2\sum_{i=1}^{n}\rho_i h_i}}\right]^{+1/3} \qquad (3)$$

where

$$R_f(\phi) = \left[\frac{3\,E_T\,K_{(m)}}{4\pi g \sum_{i=1}^{n}\rho_i h_i}\right]^{1/3}$$

E_T = total energy of the explosion

$K_{(m)}$ = empirical constant of the medium in which the cavity is located

$\rho_{(m)}$ = density of the medium in which the cavity is located

$\sum_{i=1}^{n}\rho_i h_i$ = summation of the product of the density and thickness of each layer of the overburden above the explosion point

$R_f(\phi)$ = cavity radius along the horizontal

Substitution of equation (3) into equation (2) results in an equation (4) that the author believes to provide the best calculated estimate of the vertical displacements at the surface caused by cavity formation.

$$\Delta V = \left\{ R_f(\phi) \left[1 - \frac{\rho_{(m)} \, R_f(\phi) \sin\theta}{2 \sum_{i=1}^{n} \rho_i h_i} \right]^{-1/3} \right\}^3 \sin\theta \qquad (4)$$

$$3 \left[R_i(\theta) \right]^2$$

Surface vertical displacements due to faulting were calculated using dislocation theory equations derived and programmed for use on an IBM 7094 computer by Frank Press (written commun., 1965). The present author modified this program to run on a CDC 3600 computer and he used printout from this program in the following analysis.

Derivation of model

Downward vertical displacement at the stations owing to cavity collapse has been eliminated from consideration; therefore, the measured vertical displacement at the stations is assumed to be caused by cavity formation and faulting. Figure 4, which is a diagram of measured surface vertical displacement versus radial distance from the origin of the mathematical fault model on F-1 to the stations, indicates that a discontinuity of displacement across fault F-1 exists.

Upward displacements roughly radially symmetrical to GZ can be accounted for by assuming that there was doming over the explosion.

If doming of the area around GZ were the only cause of displacement at the stations there would be no discontinuity of displacement across fault F-1.

The discontinuity of displacement across fault F-1 can be explained using dislocation theory. The measured displacements at the stations may be explained by adding together the theoretical displacements calculated for faulting and cavity formation.

Surface vertical displacements due to cavity formation are calculated using equation 4. Results of the calculation of equation (4) for each

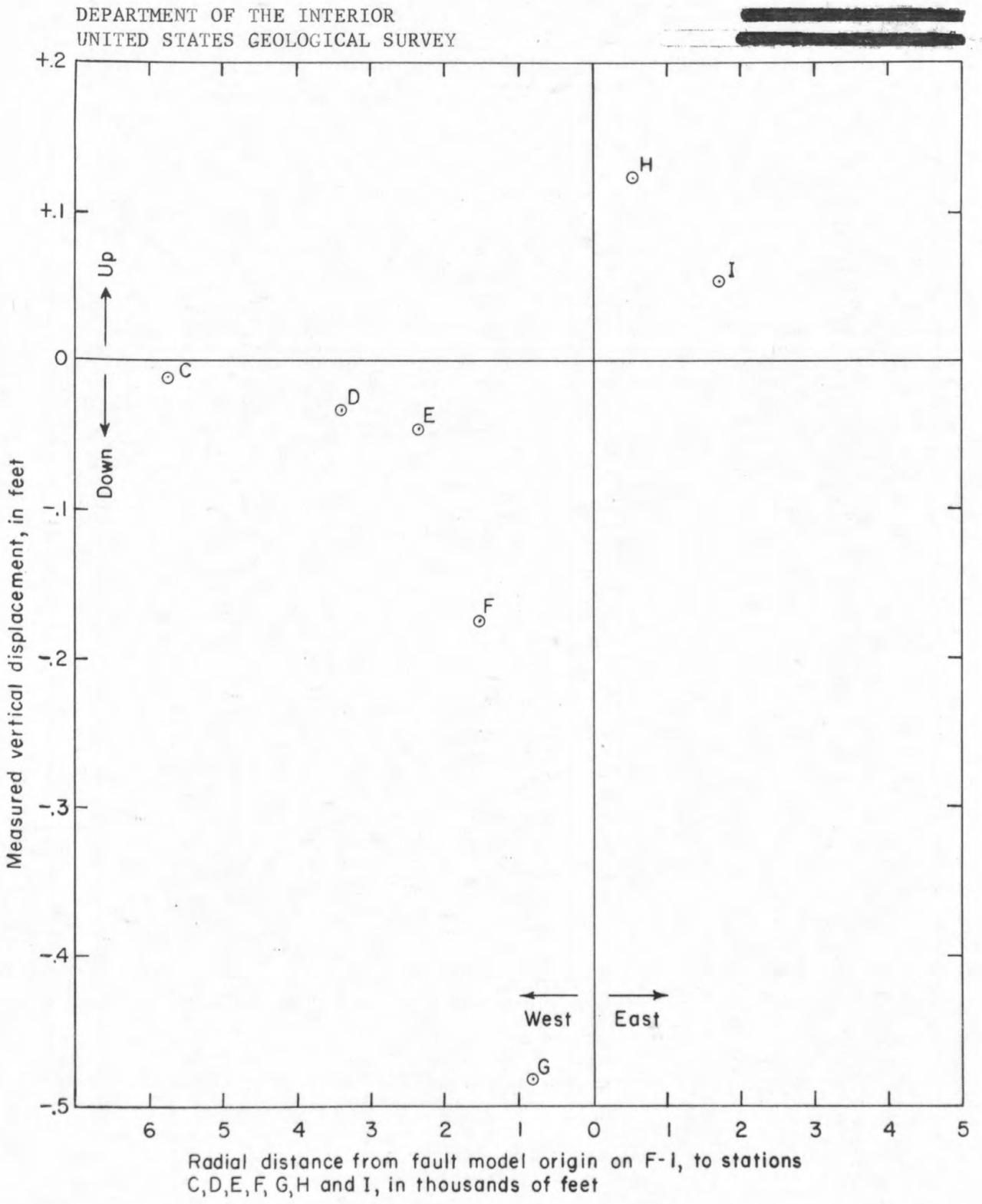

Figure 4.--Measured vertical displacements at level-line stations C, D, E, F, and G which are west of fault F-1 and stations H and I which are east of fault F-1.

station are shown in table 1. The value of ΔV for each station is plotted against radial distance from GZ in figure 5. Stations A, B, J, K, L, and M were omitted in this analysis because either or both measured and theoretical displacements at these stations were too small to be meaningful at this level of accuracy. The residual displacement is the amount of displacement that must be explained by a suitable fault model.

The parameters of a mathematical fault model from which displacements may be calculated are best obtained from field studies of the geology. A vertical dip slip fault is assumed.

A zone of fractures along fault F-1 (fig. 2), a few feet wide and with a strike length of about 2,000 feet, was caused by the Duryea explosion. The fracturing may be reasonably inferred to extend another 400 feet north to a point due east of GZ. The fault model used in dislocation theory assumes that the entire length of the fault plane, 2 L, moves. Thus a fault model whose strike length is 2,400 feet could be assumed to fit the observed length of movement along F-1. The midpoint of the zone of fracturing along F-1 when projected to the surface would be the origin of the fault model. The depth below the surface to the top of the fault, DLIT, is zero because fracturing occurs at the surface along F-1.

The depth below the surface to the bottom of the fault plane, DBIG, and the dislocation of the fault plane, W_W (dislocation on the west side of the fault plane) or W_E (dislocation on the east side of the fault plane) are unknowns.

The analyses below use the known fault parameters, DLIT and L, and the displacements calculated at certain points to calculate the values of DBIG, W_W, and W_E.

Preliminary analysis of stations west of fault F-1

Station G is assumed to be the most ideal station under consideration because it is close to GZ and fault F-1 and because there are no intervening faults between GZ and station G or fault F-1 and station G.

Table 1.--Theoretical vertical displacement due to cavity formation, measured vertical displacement, and residual vertical displacement at stations on the level-line

Station (west to east along level-line)	Radial distance from GZ (feet)	Theoretical vertical displacement due to cavity formation (feet)	Measured vertical displacement (feet)	Residual vertical displacement[1/] (feet)
A	6,750	+.008	+.002	-.006
B	6,350	+.010	+.006	-.004
C	5,450	+.014	+.010	-.004
D	3,650	+.041	-.032	-.073
E	2,625	+.086	-.045	-.131
F	1,710	+.182	-.174	-.356
G	1,025	+.315	-.482	-.797
H	1,180	+.281	+.124	-.157
I	2,170	+.124	+.054	-.070
J	3,450	+.047	-.004	-.051
K	4,765	+.021	-.008	-.029
L	5,950	+.011	+.002	-.009
M	6,150	+.010	+.014	-.004

[1/] Residual vertical displacement equals measured vertical displacement minus theoretical vertical displacement due to cavity formation.

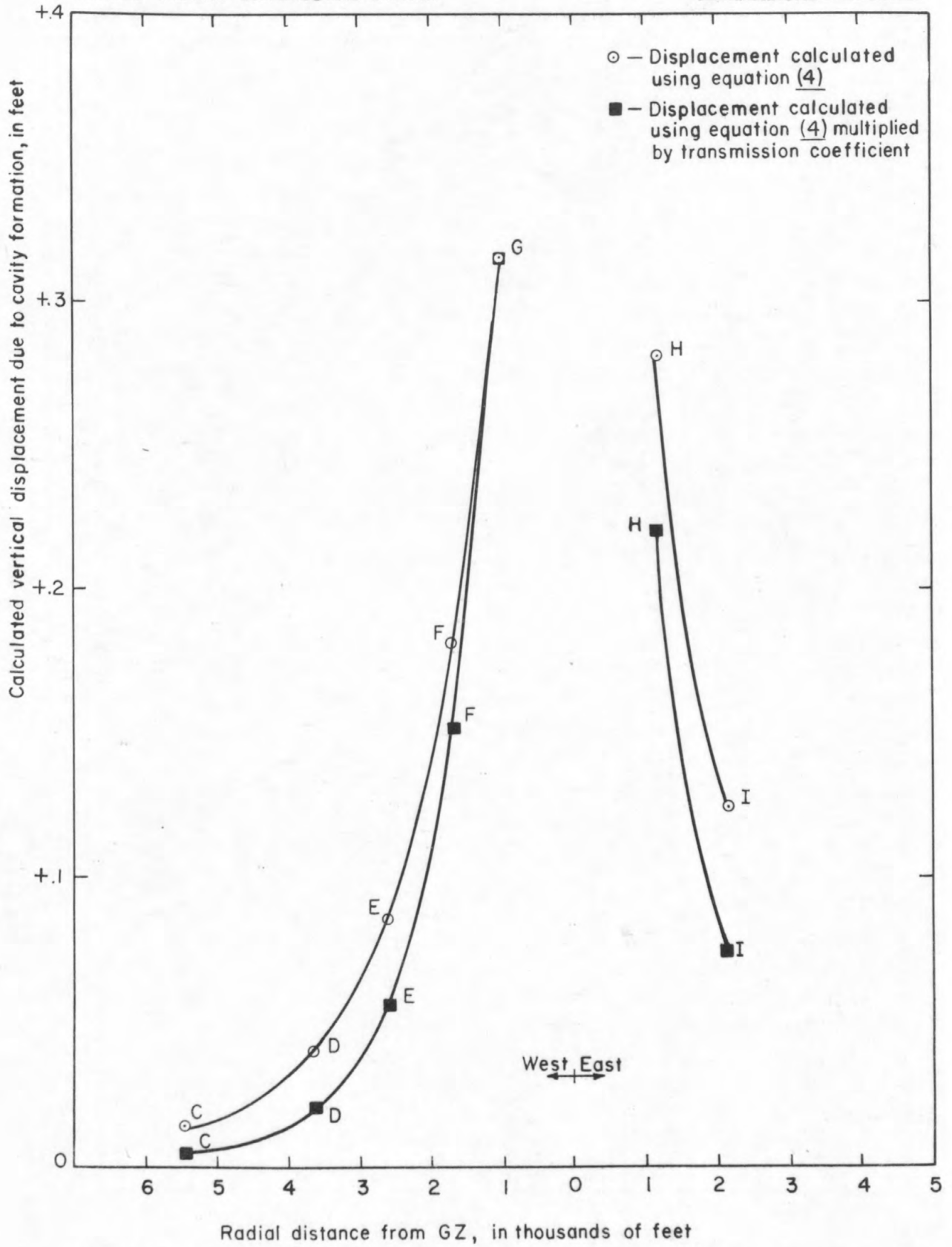

Figure 5.--Calculated vertical displacement due to cavity formation for the level-line stations D, E, F, G, H, and I using (1) equation and (2) equation--multiplied by the station transmission coefficient.

The line connecting station G and GZ is parallel to the dominant direction of fracture in this area and thus represents the most structurally homogeneous path from GZ to any station. The dislocation, W_W, of the west side of the fault can be calculated for different DBIG assuming the residual displacement at station G is due entirely to fault motion.

A value for DBIG is assumed and the theoretical value of (W/WO) for station G is calculated for this particular fault model. W is the theoretical displacement at station G and WO is the vertical dislocation across the fault model fault plane. This analysis will only investigate movement on one side of the fault at a time. Thus the fraction of theoretical displacement that will be used at all stations west of F-1 will be (W/1/2 WO) = 2(W/WO) = (W/W_W). The residual vertical displacement at station G is known and this displacement will be termed ΔV_R. At station G, for a certain assumed fault model, W = ΔV_R.

Three fault models will be tested; each will have L = 2,400 and DLIT = zero in common. The first model will assume DBIG = 1.5 L, the second model will assume DBIG = 2.0 L, and the third model will assume DBIG = 3.0 L. At station G, ΔV_R = -0.797.

At station G

Model 1: DBIG = 1.5 L : (W/WO) = .2159 : (W/W_W) = .4318

Model 2: DBIG = 2.0 L : (W/WO) = .2470 : (W/W_W) = .4940

Model 3: DBIG = 3.0 L : (W/WO) = .2967 : (W/W_W) = .5934

Solving for W_W we find the following values for the three models used in attempting to explain displacements west of F-1.

Model 1: DBIG = 1.5 L W_W = -1.85 feet

Model 2: DBIG = 2.0 L W_W = -1.61 feet

Model 3: DBIG = 3.0 L W_W = -1.34 feet

Using these models and Press' dislocation method (1965) the residual vertical displacements for all stations west of F-1 can be calculated and are shown with the residual vertical displacements from table 1, in table 2. Figure 6 is a plot of these data. Inspection of figure 6 and table 2 leads to the conclusion that 1.5 L $\leq$ DBIG $\leq$ 2.0 L.

Table 2.--Residual vertical displacements calculated from dislocation theory compared with residual vertical displacements from table 1

Station	Distance from F-1	Residual vertical displacement from table 1 (feet)	Residual vertical displacement calculated from dislocation theory (feet)		
			Model 1 DBIG = 1.5 L	Model 2 DBIG = 2.0 L	Model 3 DBIG = 3.0 L
G	832	-.797	-.797	-.797	-.797
F	1,530	-.356	-.318	-.387	-.426
E	2,360	-.131	-.120	-.166	-.222
D	3,405	-.073	-.040	-.063	-.105
C	5,745	-.004	-.006	-.012	-.026

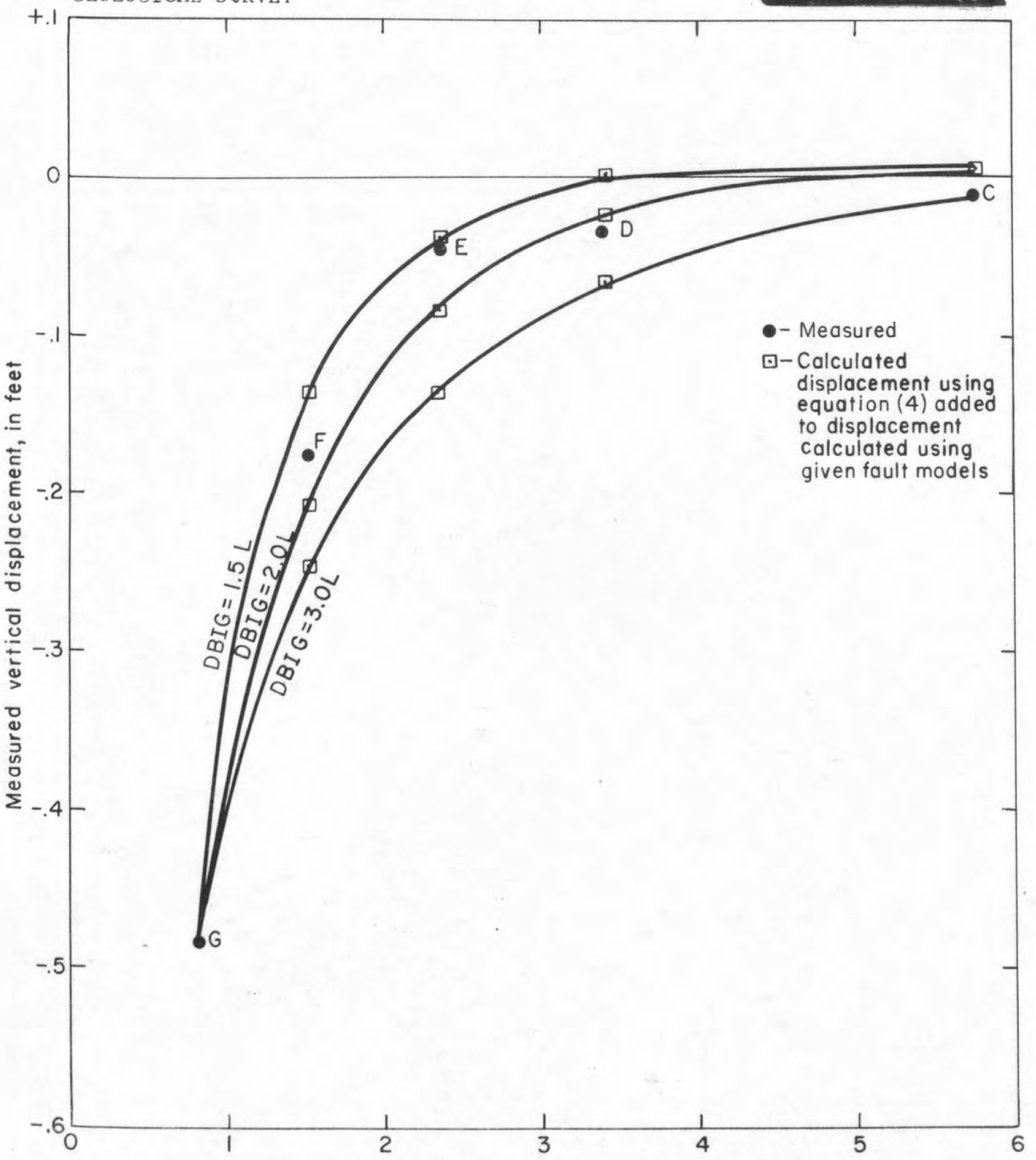

Figure 6.--Measured vertical displacements and calculated vertical displacements using equation (4) added to calculated vertical displacements using given fault models for stations west of fault F-1.

Analysis of stations east of fault F-1

The measured vertical displacements at stations H and I are assumed to be equal to the vertical displacement produced by cavity formation plus the vertical displacement produced by dislocation, W_E, at fault F-1. In equation form this would be

At station H

$$+.124 = X_H \Delta V_H + 2(W/WO)^H_{DBIG}\, W_E \tag{5}$$

and at station I

$$+.054 = X_I \Delta V_I + 2(W/WO)^I_{DBIG}\, W_E \tag{6}$$

where

X_H = a transmission coefficient of displacement for path from explosion point to station H

ΔV_H = vertical displacement of point H due to cavity formation

$X_H \Delta V_H$ = modified displacement due to cavity formation

$2(W/WO)^H_{DBIG}$ = fraction of vertical dislocation at station H due to a fault with assumed DBIG and dislocation W_E

W_E = dislocation on east side of fault

Equations (5) and (6) can be combined using simultaneous equations method to form

$$.124(W/WO)^I_{DBIG} - X_H \Delta V_H (W/WO)^I_{DBIG} - .054(W/WO)^H_{DBIG} + X_I \Delta V_I (W/WO)^H_{DBIG} = 0 \tag{7}$$

Equations (5), (6), and (7) cannot be solved unless W_E or X_H or X_I are known.

Let us examine what we know about these unknowns.

$$\left.\begin{aligned} 0 \le X_H \le 1 \\ 0 \le X_I \le 1 \end{aligned}\right\} \tag{8}$$

$$W_E \ge 0 \tag{9}$$

The problem is that there are two equations in three unknowns. These equations cannot be solved uniquely if all three of the unknowns are independent. It is probable that X_H and X_I are functionally related since both are transmission coefficients.

Values for W_E and X_I can be calculated using equations (5) and (6) by assuming values for X_H and DBIG. Values for X_I can also be calculated using equation (7) by assuming values for X_H and DBIG. The values used for DBIG will be 1.5 L and 2.0 L which were obtained in the preliminary analysis of the stations west of fault F-1. The values assumed for X_H will be one and zero, the two extreme values for this unknown. To find values for X_H and W_E, values of one and zero can be assumed for X_I. Values for X_I and X_H can be calculated assuming W_E equals zero. The results of the calculation of equations (5) and (6) with the assumptions given above are tabulated in table 3. Model 5 in table 3 can be eliminated from consideration because the calculated transmission coefficients X_H and X_I are approximately equal. The coefficients could only be equal if the path from GZ to station H and the path from GZ to station I were both homogeneous and of equal length or both paths showed equal transmission of displacement. Figure 2, however, shows obvious differences in structure along the paths from GZ to the two stations; furthermore, the slant distance from the explosion or working point, WP, to station H is 2,150 feet compared to 2,830 feet from the WP to station I.

It is logical to assume that a path perpendicular to the direction of dominant fracturing will result in a smaller transmission coefficient than a path parallel to the direction of dominant fracturing. The path from the WP to station I is more nearly perpendicular to the direction of dominant fracturing for this area than the path from the WP to station H.

Models 1 and 2 in table 3 are then eliminated because $X_H < X_I$ for these models, which is inconsistent with the preceding logic.

This leaves models 3 and 4 in table 3 acceptable; however, these models must be modified by some functional relationship between X_H and X_I because it is probable that $X_H \neq 1.0$.

A simple modification would be to assume that

$$X_H SL_H = X_I SL_I \qquad (10)$$

Table 3.--Transmission coefficients and displacement models for stations east of fault F-1

Model	DBIG(L)	X_H	X_I	W_E (feet)
1	*1.5	*0.0	0.226	+0.180
2	*2.0	*0.0	0.157	+0.171
3	*1.5	*1.0	0.701	-0.228
4	*2.0	*1.0	0.788	-0.217
5	----	0.442	0.446	*0.0

*Assumed values

where SL_H and SL_I are the distances from WP to stations H and I, respectively. Upon substituting the values of SL into equation (10) the equation results in

$$\frac{X_H}{X_I} = 1.31 \tag{11}$$

By using equation (7), X_I can be computed for a given X_H and the ratio of $\frac{X_H}{X_I}$ for DBIG = 1.5 L and DBIG = 2.0 L can be calculated. The results of these calculations are shown in table 4.

From table 4 it is seen that the ratio for model 2 and DBIG = 1.5 L is closest to the value given in equation (11). Thus a fault model with DBIG = 1.5 L would be most acceptable to explain displacement at stations east of F-1 and also must be the most acceptable DBIG for a fault model to explain displacement at stations west of F-1.

Substitution of equation (11) into equation (7) results in a model for the displacement as follows:

DLIT = 0	DBIG = 1.5 L	East model
L = 1,200 feet	W_E = -0.14 feet	
X_H = 0.784	X_I = 0.598	

The calculated residual vertical displacements at stations west of F-1 must be modified by transmission coefficients for each station according to the path direction and path length to each station. Using equation (10) in the form

$$X_{(i)}\ SL_{(i)} = X_{(G)}\ SL_{(G)} \tag{12}$$

where

(i) = F, E, D, and C

and assuming $X_{(G)} = 1.0$, the transmission coefficients can be computed.

The model for the displacements at the stations west of F-1, therefore, becomes

DLIT = 0	DBIG = 1.5 L	West model
L = 1,200 feet	W_W = -1.85 feet	
X_G = 1.0	X_F = 0.834	
X_E = 0.651	X_D = 0.509	
X_C = 0.361		

Table 4.--Ratio of transmission coefficients for stations H and I

Model	DBIG = 1.5 L			DBIG = 2.0 L		
	X_H	X_I	X_H/X_I	X_H	X_I	X_H/X_I
1	.900	.654	1.37	.900	.725	1.24
2	.800	.606	1.32	.800	.662	1.21
3	.700	.558	1.25	.700	.598	1.17
4	.600	.511	1.17	.600	.536	1.12
5	.500	.463	1.08	.500	.473	1.06
6	.400	.416	0.96	.400	.410	0.98

The modified calculated vertical displacements due to cavity formation are shown in figure 5.

By using the east and west models the calculated surface vertical displacements can be compared with measured surface vertical displacements as shown in table 5 and figure 7.

Summary

In this analysis the asymmetrical vertical displacements at seven stations are explained by using a combination of displacements calculated from dislocation theory and cavity formation. Upward displacement due to cavity formation is modified in accordance with the effects of geologic structure on the transmission of displacement in different directions. The strike length of fault F-1 and the origin of the coordinate system set up on F-1 were based upon geologic mapping of explosion-produced fracturing. The final fault model required by dislocation theory to predict the displacement due to faulting has the following dimensions:

1. Depth to bottom of fault plane: 1,800 feet
2. Depth to top of fault plane; 0 feet
3. Strike length of fault plane: 1,200 feet
4. Dislocation on west side of fault F-1: -1.85 feet
5. Dislocation on east side of fault F-1: -0.14 foot

It is evident from the measured vertical displacement that displacement resulting from faulting must be considered in conjunction with the displacement produced by cavity formation to explain the displacement at the stations.

Table 5.--Calculated vertical displacements and measured vertical displacements

Station (from west to east)	Calculated vertical displacement (feet)			Measured displacement (feet)
	From cavity formation	From fault model	Algebraic sum	
C	+.005	-.006	-.001	-.010
D	+.021	-.040	-.019	-.032
E	+.056	-.119	-.063	-.045
F	+.152	-.317	-.165	-.174
G	+.315	-.797	-.482	-.482
H	+.220	-.096	+.124	+.124
I	+.074	-.020	+.054	+.054

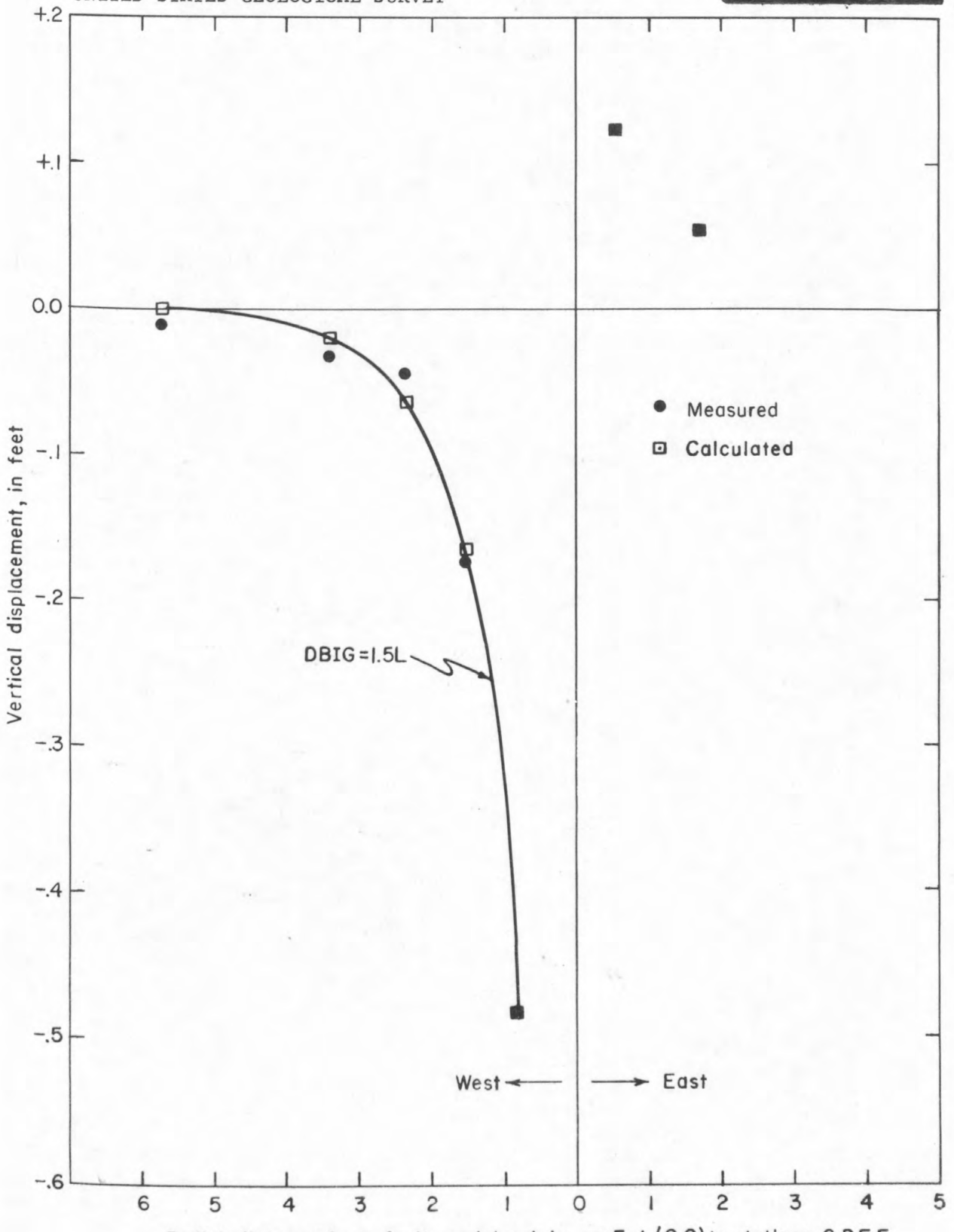

Figure 7.--Measured displacement and calculated displacement for stations C, D, E, F, G, H, and I

References cited

Brethauer, G. E., 1968, Calculation of cavity radius using an average potential energy function: U.S. Geol. Survey open-file report.

Byers, F. M., Jr., and Cummings, David, 1967, Geologic map of the Scrugham Peak quadrangle, Nye County, Nevada: U.S. Geol. Survey Geol. Quad. Map GQ-695.

Ekren, E. B., 1966, Geologic map of the Silent Butte quadrangle, Nye County, Nevada: U.S. Geol. Survey Geol. Quad. Map GQ-493.

Press, Frank, 1965, Displacements, strains, and tilts at teleseismic distances: Jour. Geophys. Research, v. 70, no. 10, p. 2395-2412.

U. S. GEOLOGICAL SURVEY
Washington, D. C.
20242

For release MAY 27, 1968

The U. S. Geological Survey is releasing in open files the following reports. Copies are available for consultation in the Geological Survey Libraries, 1033 GSA Bldg., Washington, D. C. 20242; Bldg. 25, Federal Center, Denver, Colo. 80225; and 345 Middlefield Rd., Menlo Park, Calif. 94025. Copies are also available for consultation in other offices as listed:

1. Geologic maps, structure sections, and fence diagrams of Rangeley and Phillips quadrangles, Franklin and Oxford Counties, Maine, and heavy metals content of stream sediment samples from the Rangeley and parts of the Phillips and Rumford quadrangles, Maine, by Robert H. Moench. 7 sheets, scale 1:62,500. 80 Broad St., Boston, Mass. 02110; Maine Geological Survey, 211 State Office Bldg., Augusta, Me. 04330. Material from which copy can be made at private expense is available in the Boston office.

2. Preliminary interpretation of a seismic-refraction profile across the Large Aperture Seismic Array, Montana, by C. A. Borcherdt and J. C. Roller. 53 p., including text, 2 figs., and 26 p. tabular material.

The following reports are also being released in open file. Copies of Items 3 through 7 are available for consultation in the Geological Survey Libraries, 1033 GSA Bldg., Washington, D.C. 20242; Bldg. 25, Federal Center, Denver, Colo. 80225; 345 Middlefield Rd., Menlo Park, Calif. 94025; 1012 Federal Bldg., Denver, Colo. 80202; 8102 Federal Office Bldg., Salt Lake City, Utah 84111; 504 Custom House, San Francisco, Calif. 94111; 7638 Federal Bldg., Los Angeles, Calif. 90012; and Library, Mackay School of Mines, University of Nevada, Reno, Nev. 89507:

3. Timber Mountain Tuff, southern Nevada, and its relation to cauldron subsidence, by F. M. Byers, Jr., Paul P. Orkild, W. J. Carr, and W. D. Quinlivan. 23 p., 11 figs.

4. Silent Canyon volcanic center, Nye County, Nevada, by Donald C. Noble, K. A. Sargent, H. H. Mehnert, E. B. Ekren, and F. M. Byers, Jr. 20 p., 4 figs., 2 tables.

5. Subsurface geology of the Silent Canyon caldera, Nevada Test Site, Nevada, by Paul P. Orkild, F. M. Byers, Jr., D. L. Hoover, and K. A. Sargent. 19 p., 7 figs.

6. Application of dislocation theory to analysis of vertical displacements at the ground surface caused by the Duryea Event, by G. E. Brethauer. 24 p., 7 figs., 5 tables.

7. Calculation of cavity radius using an average potential energy function, by G. E. Brethauer. 20 p., 3 figs., 1 table.